Cross-References

- ▶ Acoustic Trapping
- ▶ Acoustophoresis
- ▶ Integrated Micro-acoustic Devices

References

1. Gorkov L.P.: On the forces acting on a small particle in an acoustical field in an ideal fluid. Soviet Physics Doklady (**6**), 9, 773–775 (1962)

Acoustic Nanoparticle Synthesis for Applications in Nanomedicine

Aisha Qi, Peggy Chan, Leslie Yeo and James Friend
Micro/Nanophysics Research Laboratory,
RMIT University, Melbourne, VIC, Australia

Synonyms

Drug delivery and encapsulation; Nanocarriers; Nanomedicine; Polymer nanocapsules; Sound propagation in fluids; Ultrasonic atomization

Definition

Sound wave propagation arising from the high-frequency acoustic irradiation of a fluid can generate considerable stresses at the free surface of the fluid leading toward its destabilization and subsequent breakup. If the fluid comprises a polymer solution, the evaporation of the solvent from the aerosols that are generated as a consequence of the atomization process leaves behind a solidified polymer core with submicron dimensions. Here, any discussion of nanoparticle synthesis due to chemical reactions driven by sound waves, i.e., sonochemistry, is omitted and the discourse is limited to the physical synthesis of such nanoparticles due to the atomization of polymer solutions into a gas, typically dry air.

Overview

The synthesis of functional nanoparticles is an area of tremendous interest, particularly from the standpoint of many industry applications from catalysis, optics, and electronics to biomolecular sensing, regenerative medicine, and pharmaceutical science. In the latter, there are several challenges that current drug delivery technologies and systems face. For example, the low solubility of many drugs in biological environments prevents their absorption and distribution in vivo [1, 2]. While drug solubility limitations can be circumvented through chemical structure modification or the introduction of surfactant, the former often requires expensive and complicated procedures whereas the latter may not only increase the dosage volume but is also associated with toxicity problems [1]. In addition, the delivery of most drugs cannot be localized to target a site of interest, leading to undesirable side effects or immune responses when taken up by uninfected tissues and organs. Further, drugs are often susceptible to decomposition, enzymatic degradation, aggregation, or denaturation, thus either reducing their shelf life or their efficacy in vivo.

Nanoparticle-based delivery systems, however, offer the possibility of addressing some of these issues. For example, the drug dissolution rate can be increased by reducing the particle size [1, 2]. Tumor tissues are characterized by leaky vasculature and poor lymphatic clearance; due to their subcellular dimensions, nanoparticles are able to preferentially accumulate in tumor tissue through an enhanced permeation and retention (EPR) effect [3]. As an attractive alternative to conventional invasive surgical procedures, nanoparticles have also been reported to be able to cross the blood–brain barrier to be administrated into the central nervous system [1].

The encapsulation of drugs within the polymer nanoparticle not only acts as a protective layer surrounding the drug from hostile in vivo environments but also enables the drug to diffuse out slowly over extended periods. Such controlled release as well as direct local targeting of diseased regions can also be further tuned by judicious choice of the polymeric excipient chemistry, comonomer ratios, and their degradability in certain regions. Further site-specific targeting can be achieved by functionalizing the nanoparticle surface with tissue-specific or cell-specific ligands to increase uptake into receptor expressing

cells [3]. Alternatively, it is straightforward to chemically modify the nanoparticle surface to actively target a diseased site by attaching a surface-bound ligand, e.g., monoclonal antibodies or polymeric conjugates that specifically bind to target cells [1].

There are numerous routes for nanoparticle synthesis, all of which can be broadly delineated into three general approaches. Mechanical milling techniques are widely used commercially but are typically confined to industrial applications such as ceramics and paints due to contamination issues. While the level of impurities can be reduced, for example, by carrying out the process in vacuum, this is expensive and the powders are often polydispersed. Wet chemical deposition and precipitation techniques involve phase separation and include crystallization and sol-gel processing. Polymeric nanoparticles can be synthesized using emulsion (solvent extraction/evaporation) and self- or directed-assembly methods. These are usually batch operations and mass production can lead to scale up in complexity and cost. Moreover, while these methods allow for size and size distribution reproducibility, controlling these parameters is difficult. Gas phase evaporation and condensation techniques, on the other hand, encompass a range of methods that include combustion flame pyrolysis, plasma chemical vapor deposition, and laser ablation as well as spray drying. As with all aerosol processing strategies, spray drying is typically straightforward, fast, and allows high throughput, producing dried nanoparticles by atomizing a solution into micron or submicron-sized aerosols which then rapidly pass through a drying configuration. By removing the solvent either through evaporation or extraction using a hardening agent [4–6], the material of interest, e.g., proteins, peptides, and a wide range of polymers, can solidify into dried particles usually with desired dimensions and morphologies governed by the parent aerosol [7].

Other aerosol processing techniques include hydrodynamic flow focusing and electrospraying. Hydrodynamic flow focusing generates droplets by forcing liquid through an orifice using direct pressure or a fast moving air stream [8], although this typically results in an uneven and large particle size distribution. As such, it is typically used by the food industry, for example, in the manufacture of milk powder, in which stringent particle size requirements are not essential. Electrospraying, on the other hand, employs large voltages to stretch and pinch off aerosol droplets from a liquid meniscus at the tip of a metal capillary [9]. While this produces aerosol droplets and polymeric nanoparticles with a uniform size distribution, the throughput is generally low and the large electric fields required not only poses safety hazards but could also result in molecular lysis, although these could potentially be circumvented using high-frequency AC fields [10].

New technologies for nanoparticle synthesis and drug encapsulation, however, have not kept up with the rapid advances achieved in nanomedicine, particularly, from the standpoint of drug discovery and formulation. The rest of this entry is concerned with atomization processes via acoustic means for polymeric nanoparticle synthesis and recent advances in this field that allow it to be exploited as a powerful tool for drug delivery.

Ultrasonic Atomization

Ultrasonic atomization generally refers to a method for aerosol production induced by irradiating a fluid in order to destabilize its interface with acoustic energy at driving frequencies between 20 kHz to a few MHz [11], although novel technologies such as surface acoustic waves (SAWs) allow operation at higher frequencies above 10 MHz [12]. The source of the acoustic energy is usually a piezoelectric transducer driven by an alternating electrical signal. Ultrasonic atomization therefore typically encompasses both indirect and direct vibration-induced atomization [11, 13], ultrasonic microjetting [14], and, more recently, SAW atomization [15]. Figure 1 illustrates these various conceptual strategies that are generally classified as ultrasonic atomization methods, the difference between these arising through the mechanism by which the acoustic energy is introduced or the way in which the aerosol droplets are produced. For example, *bulk* vibration energy is transferred indirectly from the piezoelectric transducer to the fluid drop to be atomized through a metallic horn (Fig. 1a) or directly to the sessile fluid drop placed on the piezoelectric

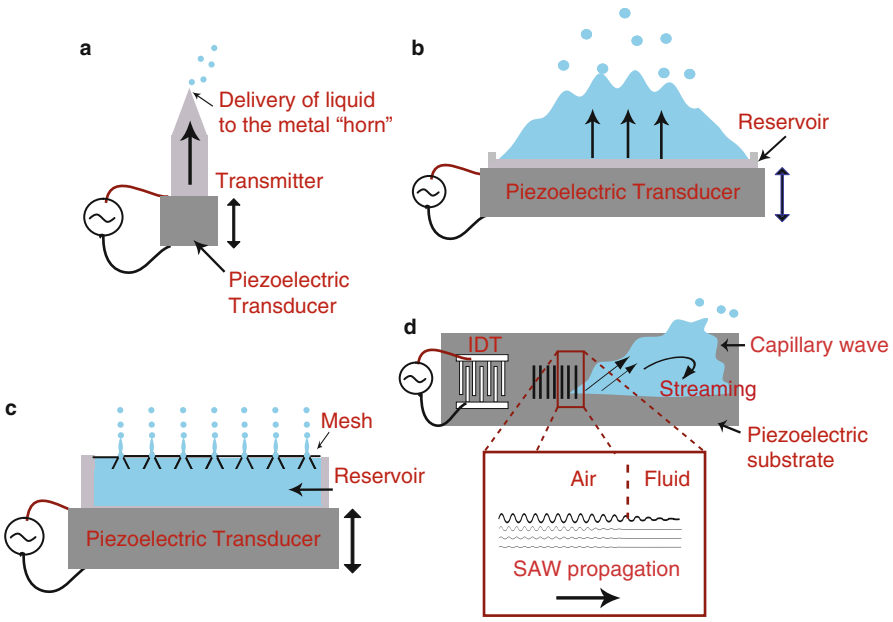

Acoustic Nanoparticle Synthesis for Applications in Nanomedicine,
Fig. 1 Different conceptual configurations for ultrasonic atomization. (**a**) Indirect bulk vibration driven by a piezoelectric transducer via a metallic horn on which the working fluid drop is deposited. (**b**) Direct bulk vibration transmitted to the fluid drop placed on the piezoelectric transducer. (**c**) Use of micron-sized nozzles and orifices to drive ultrasonic microjets. (**d**) Transmission of surface vibration energy in the form of SAWs into a fluid drop to drive interfacial destabilization

substrate (Fig. 1b). Nozzles and orifice plates from which fluid jets emanate that subsequently break up into aerosol droplets can also be used in an extension of the indirect method to provide finer control over the final droplet size (Fig. 1c). Alternatively, a nozzle can assume the place of the horn in the direct method in Fig. 1a, with the fluid issuing through the needle instead of placing the fluid on the horn. Nozzles or orifices however tend to clog over time and require constant cleaning; the pressure drop is also significantly increased, and hence more power is typically required to drive the atomization process. Alternatively, the *surface* vibration in the form of SAWs can couple acoustic energy into a fluid drop sitting on the piezoelectric substrate to effect interfacial destabilization (Fig. 1d). The operating principle and governing mechanisms that underpin ultrasonic atomization (cavitation or capillary wave destabilization) are discussed in detail in Yeo et al. [12].

The average diameter D of the aerosol droplets produced depends on the most unstable wavelength λ of the capillary wave instability that is induced, specified by the Kelvin equation, which essentially arises from a dominant force balance between the stabilizing capillary stresses and the destabilizing stress imposed by the vibration:

$$D \approx C_1 \lambda \approx C_2 \left(\frac{2\pi\gamma}{\rho f_c^2} \right)^{\frac{1}{3}}, \tag{1}$$

where γ and ρ are the surface tension and density of the fluid, respectively, and f_c is the capillary wave frequency. C_1 and C_2 are empirically determined coefficients commonly used to fit the experimental data to the predictions, and vary widely in the literature, although they are typically of order unity. It should be noted that Kelvin's theory does not provide a way in which the capillary wave frequency is related to the forcing frequency due to the acoustic vibration, and the usual assumption made (see, for example, [15]) is that the capillary waves are excited at a subharmonic frequency that is one half of the forcing frequency, i.e., $f_c = f/2$. Recent studies have however shown that this may not always be true and that the capillary wave frequency can be predicted from a dominant balance between capillary and viscous stresses, at least for a sessile drop or thick liquid film [12, 15]:

$$f_c \sim \frac{\gamma}{\mu L}, \tag{2}$$

where μ is the viscosity of the fluid and L is the characteristic length scale of the drop or film. A correction factor $(H/L)^2$, wherein H is the characteristic height scale, can be included to account for the geometry of the parent drop, in particular, the axial capillary stress, when substituting Eq. 2 into Eq. 1 [15].

SAWs, generated by applying an oscillating electrical signal to the interdigital transducer electrodes patterned onto a piezoelectric substrate (Fig. 1d), the gap and width of which specifies the SAW wavelength and hence the resonant frequency (typically 10–100 MHz), have also been shown as an effective mechanism for atomizing drops. Essentially, SAWs are nanometer order amplitude ultrasonic waves that are confined to and propagate along the substrate surface in the form of a Rayleigh wave. Owing to high MHz order frequencies and substrate displacement velocities, on the order of 1 m/s in the vertical direction perpendicular to the substrate, substrate accelerations on the order of 10^7 m^2/s arise. This, together with the strong acoustic streaming that is induced within the fluid drop placed on the substrate, leads to fast destabilization and breakup of the drop free surface to produce 1–10 μm dimension aerosol drops [15], as illustrated in Fig. 1d. One advantage of the SAW atomization over its ultrasonic counterparts is the efficient energy transfer mechanism from the substrate to the liquid – unlike bulk vibration, most of the acoustic energy of the SAW is localized within a region on the surface of the substrate about 3–4 wavelengths thick (a SAW wavelength is typically on the order of 100 μm) and is transferred to the liquid drop to drive the atomization. Consequently, it is possible to atomize fluids using the SAW at input powers of around 1 W, which is one to two orders of magnitude smaller than that required using other ultrasonic methods. Another advantage of the SAW is the high frequencies (>10 MHz) that can be assessed. The timescale associated with the period (inverse frequency) of the oscillating acoustic and electromechanical field at these frequencies is much shorter than the hydrodynamic timescale $\mu L/\gamma \sim 10^{-4}$ s as well as the 10^{-5}–10^{-6} s relaxation timescales (inverse of the strain rate) associated with shear-induced molecular lysis [12]. In addition, it is not possible to induce cavitation, which is known to cause molecular lysis, at the low powers and high frequencies associated with SAW atomization [15].

Synthesis of Polymeric Microparticles and Nanoparticles

Early work to demonstrate the possibility of synthesizing polymeric particles, albeit with micron dimensions, was reported by Tsai et al. [16] and Berkland et al. [4]. The apparatus in both studies is similar, based on concept known as two-fluid atomization. A piezoelectric transducer is used to vibrate a nozzle or orifice from which a jet comprising the working fluid issues and which subsequently suffers from Rayleigh-Plateau instabilities to break up into individual aerosol droplets. In a manner similar to the Kelvin equation given in Eq. 1, the droplet diameter is controlled by the most unstable wavelength of the axisymmetric instability, which can be predicted from a dominant force balance between the inertia imposed on the jet and the capillary stresses that stabilize it, and is a function of the diameter of the undisturbed jet, which is slightly larger than the nozzle or orifice diameter. In both cases, an external annular stream surrounding the nozzle through which the liquid jet issues is employed. The annular sheath fluid consists of air in the former and an immiscible carrier liquid that does not dissolve the polymer solution in the latter. In both cases, the sheath fluid, whether air or a second immiscible liquid, is flowed much faster than the jetting fluid although the underlying reason provided for its necessity differs. In the former, the airflow is suggested to vibrate in resonance with the vibrating nozzle due to the coaxial annular arrangement, resulting in a magnification of the amplitude of the capillary waves on the liquid jet. In the latter, the interfacial shear imposed by the carrier fluid surrounding the jet is suggested to aid the primary breakup of the jet away from its parent fluid at the orifice, allowing the production of droplets one order of magnitude smaller. 40 μm diameter xanthan gum particles were synthesized in the former when driven at a fundamental resonant frequency of 54 kHz through a 0.93 mm nozzle whereas 5–500 μm diameter poly(D,L-lactic-*co*-glycolic acid) (PLGA) particles (Fig. 2) were synthesized in the latter when driven at frequencies between 19 and 70 kHz through 60 and

100 μm diameter orifices. The carrier fluid, poly(vinyl alcohol), in which the PLGA particles were collected and solidified within, however, remained on the surface of the particles, which could potentially affect physical and cellular uptake [3].

Forde et al. [17] subsequently showed the possibility of synthesizing poly(ε-caprolactone) (PCL) *nano*particles around 200 nm in dimension by atomizing a PCL/acetone solution using the direct method shown in Fig. 1b involving a piston-vibrated hard lead zirconate titanate piezoelectric disk between 1 and 5 MHz, as illustrated in Fig. 3. The nanoparticle diameter D_p can be estimated from volume considerations [18]:

$$D_p \approx D\left(\frac{C}{\rho}\right)^{\frac{1}{3}}, \tag{3}$$

wherein C denotes the initial polymer concentration, such that it is possible to tailor the nanoparticle size by tuning the aerosol size through its physical properties as well as the geometry of the parent drop, as suggested by Eq. 2.

Polymeric nanoparticles have also been produced using SAW atomization. Friend et al. [19] demonstrated the synthesis of 150–200 nm clusters of 5–10 nm PCL nanoparticle aggregates, as shown in Fig. 4, the cluster size being weakly dependent on several parameters such as the surfactant used and the drying length. The grape-bunch-like cluster morphology was attributed to nonuniform solvent evaporation during in-flight drying of the droplets that drive a thermodynamic instability. This results in spinodal decomposition and phase separation, which gives rise to separate regions that are polymer-rich and solvent-rich. The polymer-rich regions then solidify more rapidly, creating nucleation sites that lead to the formation of a cluster of PCL molecules until a critical nucleation size is attained, estimated from classical nucleation theory to be around 10 nm and consistent

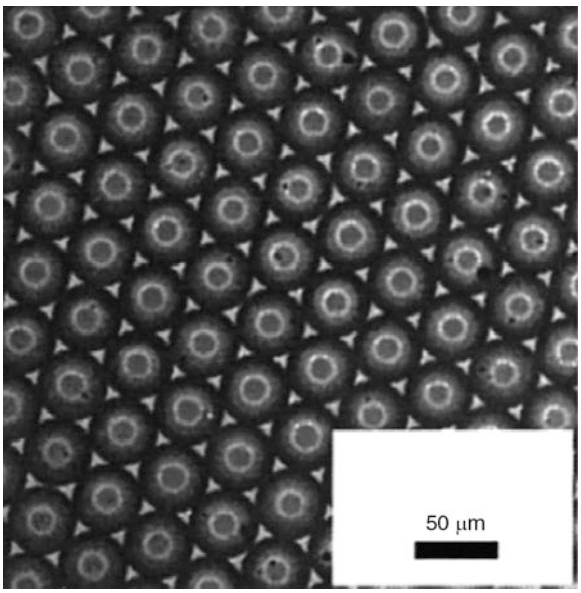

Acoustic Nanoparticle Synthesis for Applications in Nanomedicine, Fig. 2 45 μm PLGA microparticles synthesized by ultrasonically atomizing the polymer solution through a 60 μm orifice which is indirectly vibrated using a piezoelectric transducer at frequencies between 19 and 70 kHz (Reprinted with permission from Berkland et al. J. Control. Release 73, 59–74 (2001). Copyright (2001) Elsevier)

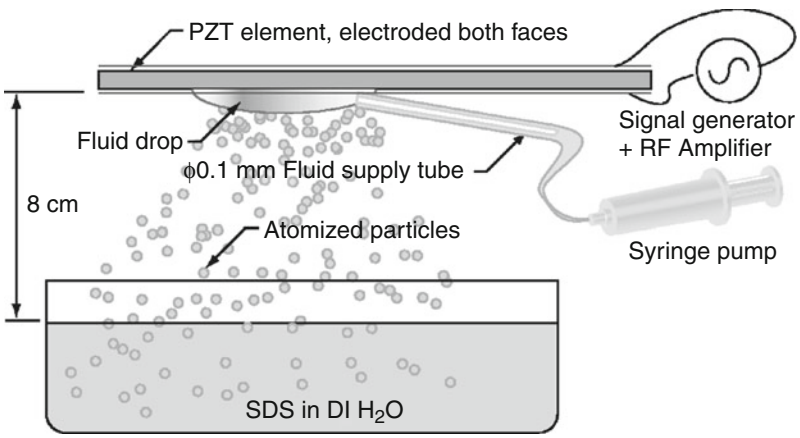

Acoustic Nanoparticle Synthesis for Applications in Nanomedicine, Fig. 3 Schematic illustration of the direct ultrasonic atomization setup of Forde et al. in which a sessile drop is vibrated at 1.645 MHz or 5.345 MHz in a piston-like manner using a hard PZT disk (Reprinted with permission from Forde et al. Appl. Phys. Lett. 89, 064105 (2006), Copyright (2006) American Institute of Physics)

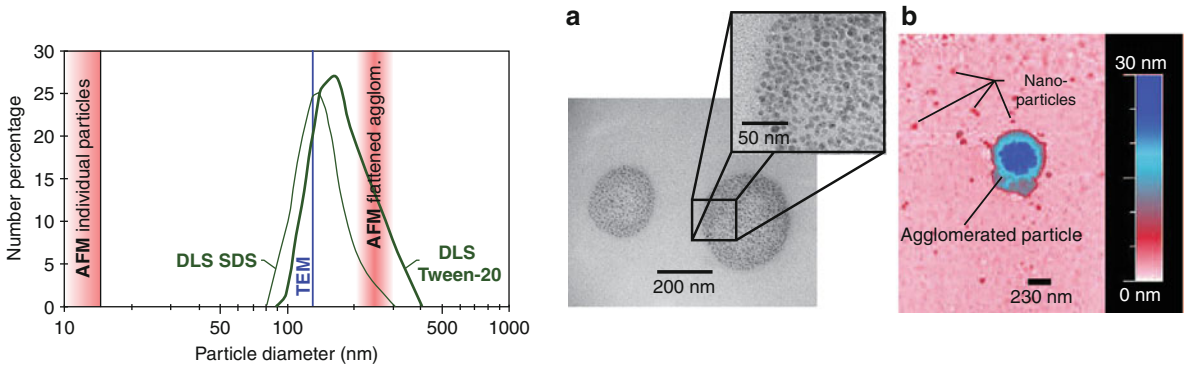

Acoustic Nanoparticle Synthesis for Applications in Nanomedicine, Fig. 4 The *left panel* shows dynamic light scattering measurements of the PCL nanoparticles produced using SAW atomization. The right panel shows (**a**) transmission electron microscopy and (**b**) atomic force microscopy images showing 150–200 nm clusters of 5–10 nm nanoparticles (Reprinted with permission from Friend et al. Nanotechnology 19, 145301 (2008). Copyright (2008) Institute of Physics)

with the 5–10 nm nanoparticles observed. In addition to PCL, 1–10 μm dimension protein (bovine serum albumin and insulin) aerosols have been generated using the SAW, which evaporate in flight to form 50 to 100 nm nanoparticles [18].

Drug Encapsulation

Early work on drug encapsulation via ultrasonic atomization was carried out by Felder et al. [5], who showed the possibility of encapsulating protein and peptides into poly(lactic acid) (PLA) and PLGA directly using ultrasonic atomization. The polymer solution was sonicated with a protein (bovine serum albumin; BSA) or peptide solution (2–10% w/w concentration) to create a stable water-in-oil emulsion, which was then atomized into a beaker in which hardening agent (octamethylcyclotetrasil, hexane, isopropyl myristate, or water) was agitated to yield 10–100 μm order microparticles. This solidification method relies on *solvent extraction* and hence polymer desolvation within the hardening agent as opposed to *solvent evaporation* in-flight used in the other methods reported here. While smaller nanoparticles on the order of 100 nm diameter were also reported, it is not clear whether these contained any encapsulated material, as the authors only reported size distribution data for the naked PLA and PLGA particles. It would, however, be consistent with the other studies reported below that encapsulated particles are generally of micron-order dimension due to the size of the peptides and proteins within. The frequency at which the ultrasonic atomization was carried out was also unspecified. Reported encapsulation efficiencies, obtained by dissolving the polymer particles in the original solvent (or an acetonitrile/chloroform mixture) to release the encapsulated material which is then recovered on a 200 nm cellulose filter followed by elution with phosphate buffered saline and quantitative characterization using a spectrofluorometer (protein) or through a HPLC assay (peptides), were typically low, between 10% and 35%. This was attributed to comparable extraction rates between that of the aqueous phase in which the protein or peptide resides with that of the polymer solvent through diffusion and partitioning. Consequently, the protein or peptide is removed during washing. When a different peptide which is only weakly soluble in water was encapsulated, the efficiency was observed to increase to 63% and 93%. As such, it is instructive to note here that encapsulation efficiencies are therefore likely to be higher if solvent evaporation is used as the polymer desolvation method instead of solvent extraction, since the solvent is much more likely to be removed rapidly through evaporation while in flight at a rate much faster than that of water, therefore resulting in more efficient encapsulation of the aqueous phase and the

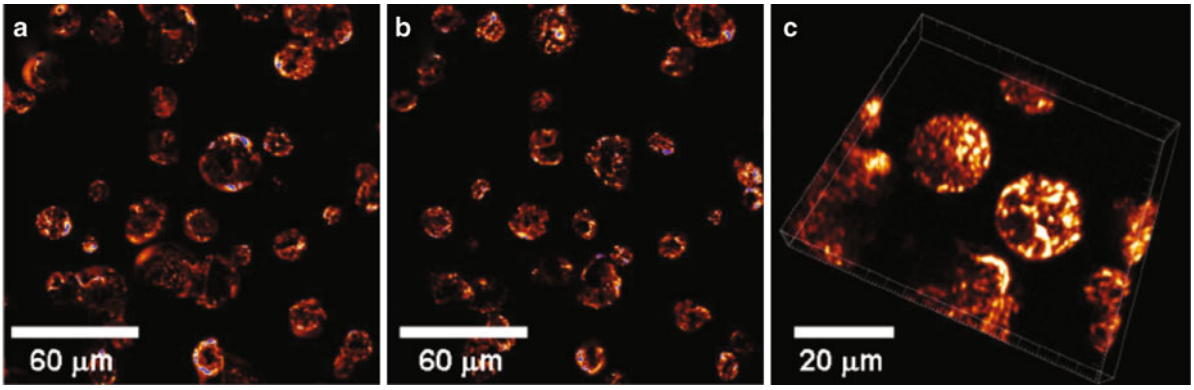

Acoustic Nanoparticle Synthesis for Applications in Nanomedicine, Fig. 5 Confocal microscope images of the cross-sectional slice (*top, bottom, and center*) across a PCL microparticle showing the encapsulation of fluorescent biotin within (Reprinted with permission from Alvarez et al. Biomicrofluidics 3, 014102 (2009). Copyright (2009) American Institute of Physics)

proteins or peptides within the fast solidifying polymer shell.

BSA was also encapsulated in PLGA using 100 kHz ultrasonic atomization of a similar water-in-oil emulsion in a study by Freitas et al. [6]. The solvent was evaporated and the solidified particles were collected and further desolvated in an agitated aqueous solution and subsequently recovered using a filter. To allow for aseptic encapsulation conditions, the conventional spray dryer unit was shortened by running the unit under near-vacuum conditions instead of using hot air, and the cyclone unit that is usually present in spray dryers was replaced by an aqueous collection bath; in that way, the entire unit can be placed within a laminar flow chamber. Again, the particles were in the micron dimension (13–24 μm mean diameter). As expected due to the use of solvent evaporation over solvent extraction, the BSA encapsulation efficiencies were higher, around 50–60% compared to 10–35%, which the authors claim could be improved if BSA loss in the aqueous collection solution was replaced by a fluid which is a nonsolvent for BSA. Alternatively, they suggest reducing the polymer concentration.

Plasmid DNA (pDNA) and poly(ethyleneimine) (PEI) complexes were encapsulated within 10–20 μm diameter PLGA microparticles using a 40 kHz ultrasonic atomizer [20]. Solvent extraction via a poly (vinyl alcohol) hardening agent was used in this case. Encapsulation efficiencies in a wide range between

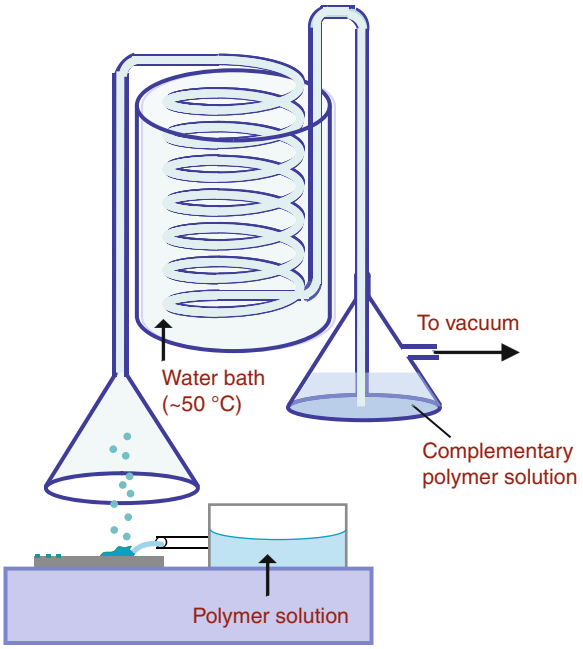

Acoustic Nanoparticle Synthesis for Applications in Nanomedicine, Fig. 6 Schematic illustration of the SAW atomization setup involving a single atomization–evaporation–resuspension step used to deposit a single polymer layer and to resuspend it in a complementary polymer solution. The step is repeated to deposit subsequent layers for as many layers as required

20% and 90% were reported, with lower polymer concentrations and higher pDNA-PEI volume fractions giving higher efficiencies; contrary to prior claims,

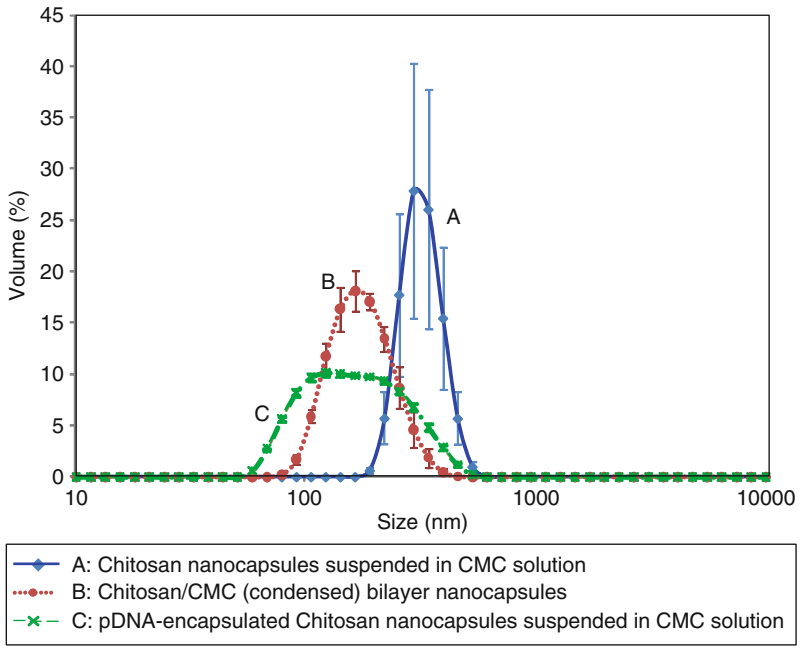

Acoustic Nanoparticle Synthesis for Applications in Nanomedicine, Fig. 7 Dynamic light scattering measurements of (**a**) single-layer chitosan nanoparticles, (**b**) bilayer chitosan and CMC nanoparticles, and (**c**) pDNA encapsulated chitosan nanoparticles

the authors however did not find significant dependence of the encapsulation efficiency on the N/P ratio (N referring to the nitrogen content and P referring to the DNA phosphate content of the pDNA-PEI complex). These values were however obtained by subtracting the mass of pDNA remaining in the hardening agent, measured using a spectrofluorometer, from that in the feedstock, which does not take into account loss of pDNA in the environment during atomization, the amount of unatomized pDNA left on the atomizer as well as the pDNA that resides on the surface of the particles instead of being encapsulated within. The authors also investigated the post-atomization structural integrity of the pDNA using gel electrophoresis due to the susceptibility of pDNA to shear degradation, and found 80% retention of the pDNA in supercoiled conformation. This was attributed to cationic complexation between pDNA and PEI, which reduces its size and hence the possibility of shear-induced degradation (when naked pDNA was assessed, only 8% of this remained supercoiled). Nevertheless, PEI has been known to induce cytotoxic effects and hence its use may be limited for gene transfection and delivery. An alternative mitigation strategy involving multilayer polymer nanoparticles will be discussed in the next section.

Alvarez et al. [18] later demonstrated the encapsulation of BSA in PCL particles using SAW

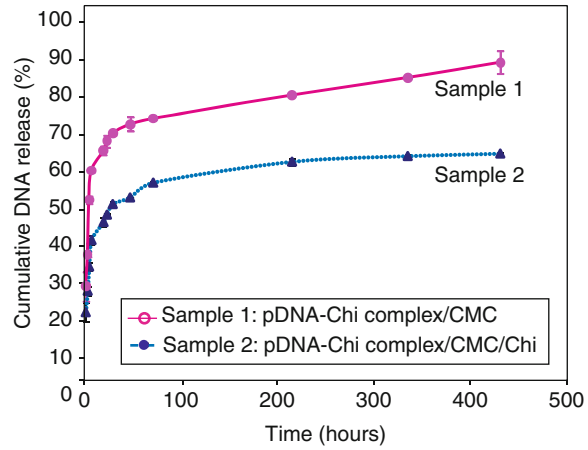

Acoustic Nanoparticle Synthesis for Applications in Nanomedicine, Fig. 8 In vitro release profile showing the diffusion of pDNA out of chitosan/CMC bilayer nanoparticles (sample 1) and chitosan/CMC/chitosan trilayer nanoparticles (sample 2) acquired through fluorescence absorbance measurements of fluorescently labeled pDNA. The lines are added to aid visualization

atomization. With 10 MHz SAWs, the particle sizes had a mean of 23 μm whereas this decreased to around 6 μm with 20 MHz SAWs. Proof of encapsulation was acquired through confocal image slices of the particles showing the fluorescently tagged BSA appearing not only at the top and bottom of the cross-sectional slices across the particle but also in the particle center,

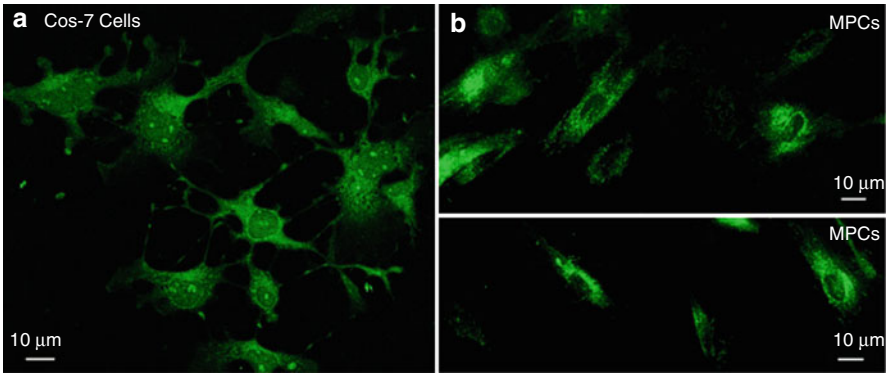

Acoustic Nanoparticle Synthesis for Applications in Nanomedicine, Fig. 9 Confocal microscopy images of (**a**) COS-7 cells and (**b**) human mesenchymal progenitor cells (MPCs) transfected with pDNA encoded with a yellow fluorescent protein (the expression is depicted in the images in *green*) encapsulated in PEI/CMC bilayer nanoparticles

thus verifying that the BSA was entrapped within and not simply bound to the surface of the particle (Fig. 5). The encapsulation efficiency value reported was slightly different compared to other studies in that 54% of BSA from the feedstock was found to be encapsulated with its chemical structure intact (as opposed to the total BSA content encapsulated reported in previous studies). Thus, the total encapsulation efficiency value could be significantly higher (if a comparison were to be made with the values in Felder et al. [5] and Freitas et al. [6]). As discussed above, the high-frequency operation of the SAW limits the amount of shear and cavitation damage caused to the molecules, and constitutes a considerable advantage of using SAWs over conventional ultrasonic atomization.

Multilayer Nanoparticle Synthesis and Encapsulation

Multilayered polymer particles offer significant advantages over a particle comprising a single layer. Layers of different polymers with varying chemistry and hence degradation profiles offer the possibility of tuning the drug release over time and in different physiological regions, therefore affording tremendous opportunities for targeted and controlled release delivery. Very recently, SAW atomization has been exploited to demonstrate the potential for rapidly synthesizing nanoparticles with alternating layers of complementary polymers of opposing charge [21]. This is done through a variation of the usual procedure of atomizing an initial polymer solution followed by evaporated-assisted solidification to produce a single-layer polymer nanoparticle. In addition, however, the solidified polymer particle is collected in a solution in which the second polymer is dissolved (Fig. 6), which is then re-atomized and dried to deposit the second polymer layer over the initial polymer core. By collecting the two-polymer-layer nanoparticle in a solution comprising the polymer to form the third layer and re-atomizing, a further layer can be deposited. The atomization–evaporation–resuspension procedure is then repeated for as many times as the number of layers desired. The requirement of the polymers comprising alternating layers is that each successive polymer must be complementary to the previous polymer, i.e., they must have opposing charges. In addition, the polymer making up the subsequent layer must be soluble in a solvent that cannot dissolve the polymer making up the previous layer. Up to eight layers of alternating chitosan (or PEI) and CMC layers were synthesized; proof of the deposition of successive layers was provided by visual inspection (atomic force microscopy), charge characterization (reversal of the zeta-potential after the deposition of each successive layer), Fourier transform infrared spectrometry showing ionic complexation between the deposited layers, and fluorescence measurements of labeled polymers. In addition, pDNA was also encapsulated within the multilayer polymeric nanoparticles to demonstrate the therapeutic capability of the nanoparticles in particular for gene therapy.

Figure 7 shows the size distribution of negatively charged chitosan and positively charged CMC polymer bilayer particles. The decrease in size upon deposition of the second CMC layer over the chitosan core or the encapsulated pDNA can be attributed to ionic complexation that tends to compact the particle size. Even with encapsulation, however, the size of the

particles remains in the 100–200 nm range, which is a significant advance over the micron-sized particles obtained whenever a therapeutic molecule is encapsulated (see previous section). In targeted cancer therapy, for example, the mean vascular pore size of most human tumors is around 400 nm [1], and hence extravasation is likely to be more effective with the multilayer nanoparticle drug carriers synthesized through this technique. Figure 8 shows in vitro release profiles of the pDNA, showing the possibility for slowing and hence controlling the release with the deposition of an additional layer. Good in vitro DNA transfection is also demonstrated in COS-7 and human mesenchymal progenitor cells, as seen in Fig. 9.

Cross-References

- ▶ Nanoencapsulation
- ▶ Nanomedicine
- ▶ Nanoparticles
- ▶ Polymer Coatings

References

1. Kumar, M.N.V.R. (ed.): Handbook of Particulate Drug Delivery. American Scientific, California (2008)
2. Mehnert, W., Mäder, K.M.: Solid lipid nanoparticles: production, characterization and applications. Adv. Drug. Deliv. Rev. **47**, 165–196 (2001)
3. Panyam, J., Labhasetwar, V.: Biodegradable nanoparticles for drug and gene delivery to cells and tissue. Adv. Drug. Deliv. Rev. **55**, 329–347 (2003)
4. Berkland, C., Kim, K., Pack, D.W.: Fabrication of PLG microspheres with precisely controlled and monodisperse size distributions. J. Control. Release **73**, 59–74 (2001)
5. Felder, C., Blanco-Prieto, M., Heizmann, J., Merkle, H., Gander, B.: Ultrasonic atomization and subsequent polymer desolvation for peptide and protein microencapsulation into biodegradable polyesters. J Microencapsul. **20**, 553–567 (2003)
6. Freitas, S., Merkle, H., Gander, G.: Ultrasonic atomisation into reduced pressure atmosphere – envisaging aseptic spray-drying for microencapsulation. J. Control. Release **95**, 185–195 (2004)
7. Alvarez, M., Friend, J., Yeo, L.Y.: Rapid generation of protein aerosols and nanoparticles via surface acoustic wave atomization. Nanotechnology **19**, 455103 (2008)
8. Gañán-Calvo, A.M.: Enhanced liquid atomization: from flow-focusing to flow-blurring. Appl. Phys. Lett. **86**, 214101 (2005)
9. Grace, J., Marijnissen, J.: A review of liquid atomization by electrical means. J. Aerosol. Sci. **25**, 1005–1019 (1994)
10. Yeo, L.Y., Gagnon, Z., Chang, H.-C.: AC electrospray biomaterials synthesis. Biomaterials **26**, 6122–6128 (2005)
11. Friend, J., Yeo, L.Y.: Microscale acoustofluidics: microfluidics driven via acoustics and ultrasonics. Rev. Mod. Phys. **83**, 647–704 (2011)
12. Yeo, L.Y., Friend, J.R., McIntosh, M.P., Meeusen, E.N.T., Morton, D.A.V.: Ultrasonic nebulization platforms for pulmonary drug delivery. Expert. Opin. Drug. Deliv. **7**, 663–679 (2010)
13. James, A.J., Vukasinovic, B., Smith, M.K., Glezer, A.: Vibration-induced drop atomization and bursting. J. Fluid. Mech. **476**, 1–28 (2003)
14. Meacham, J.M., Varady, M.J., Degertekin, F.L., Fedorov, A.G.: Droplet formation and ejection from a micromachined ultrasonic droplet generator: visualization and scaling. Phys. Fluids **17**, 100605 (2005)
15. Qi, A., Yeo, L., Friend, J.: Interfacial destabilization and atomization driven by surface acoustic waves. Phys. Fluids **20**, 074103 (2008)
16. Tsai, S.C., Luu, P., Song, Y.L., Tsai, C.S., Lin, H.M.: Ultrasound-enhanced atomization of polymer solutions and applications to nanoparticles synthesis. Trans. Ultrason. Symp. **1**, 687–690 (2000)
17. Forde, G., Friend, J., Williamson, T.: Straightforward biodegradable nanoparticle generation through megahertz-order ultrasonic atomization. Appl. Phys. Lett. **89**, 064105 (2006)
18. Alvarez, M., Yeo, L.Y., Friend, J.R., Jamriska, M.: Rapid production of protein-loaded biodegradable microparticles using surface acoustic waves. Biomicrofluidics **3**, 014102 (2009)
19. Friend, J.R., Yeo, L.Y., Arifin, D.R., Mechler, A.: Evaporative self-assembly assisted synthesis of polymeric nanoparticles by surface acoustic wave atomization. Nanotechnology **19**, 145301 (2008)
20. Ho, J., Wang, H., Forde, G.: Process considerations related to the microencapsulation of plasmid DNA via ultrasonic atomization. Biotechnol. Bioeng. **101**, 172–181 (2008)
21. Qi, A., Chan, P., Ho, J., Rajapaksa, A., Friend, J., Yeo, L.: Template-free synthesis and encapsulation technique for layer-by-layer polymer nanocarrier fabrication. ACS Nano, doi:10.1021/nn202833n

Acoustic Particle Agglomeration

- ▶ Acoustic Trapping